

## The role of surface sites on the oscillatory oxidation of methanol on Stepped Pt[n(111) x (110)] electrodes

V. Del Colle,<sup>1,2</sup> P. B. Perroni,<sup>1</sup> J. M. Feliu,<sup>3</sup> G. Tremiliosi-Filho,<sup>1</sup> H. Varela<sup>1,4,\*</sup>

<sup>1</sup>*Institute of Chemistry of São Carlos, University of São Paulo  
POBox 780, 13560-970, São Carlos, SP, Brazil.*

<sup>2</sup>*Universidade Federal de Alagoas - Campus Arapiraca, Av. Manoel Severino Barbosa  
57309-005, Arapiraca, AL, Brazil.*

<sup>3</sup>*Instituto de Electroquímica, Universidad de Alicante, Apdo. 99, E-03080 Alicante, Spain.*

<sup>4</sup>*Max-Planck Institute for the Physics of Complex Systems, Nöthnitzer Str. 38  
01187 Dresden, Germany.*

### Abstract

Reaction rates and mechanisms of most electrocatalytic reactions are known to critically depend on the structure of the electrode surface. Examples of structure sensitive electrocatalytic systems include the reduction of oxygen and the oxidation of small organic molecules on platinum, for instance. Even more intricate is the effect of the interfacial structure on the oscillatory dynamics commonly observed in some systems. This is somewhat expected because several adsorption and reaction steps are simultaneously active during self-organized potential or current oscillations. Herein we present results of the effect of surface structure on the oscillatory electro-oxidation of methanol in acidic media on Pt(111), Pt(110), and on stepped surfaces Pt(776), Pt(554), Pt(775), and Pt(332). The system was investigated at two methanol concentrations and under voltammetric and galvanostatic regimes. The voltammetric activity towards the electro-oxidation of methanol on stepped surfaces followed this sequence: Pt(776) < Pt(554) < Pt(775) < Pt(332), at high methanol concentration. The reaction rates increase with the density of (110) sites, but small (111) terraces was also found to contribute to the overall process. In terms of potential oscillations, we found specificities that were unambiguously assigned to the surface structure. In particular, the following features were found according to the specific surface studied: period-adding sequences of mixed-mode oscillations; a new type of mixed-mode oscillation; and a particular separation between two types of sequential oscillations. The understanding of the relationship between the surface structure and the underlying dynamics of the surface chemistry during oscillations is a key challenge and our findings in this direction are discussed.

**Keywords:** methanol, oscillations, electrocatalysis, platinum single crystals, stepped surfaces.

\* corresponding author (H.V.): [hamiltonvarela@usp.br](mailto:hamiltonvarela@usp.br).

## 51 1. Introduction

52

53 The electro-oxidation of methanol is an extensively studied reaction because of its  
54 importance to the interconversion between chemical and electric energies, as in the direct  
55 methanol fuel cell.<sup>1-4</sup> Many efforts have been devoted to understand how reaction rates and  
56 mechanism depends on experimental parameters such as the surface structure and composition of  
57 the electrode. The complete oxidation of methanol releases  $6e^-$  per molecule, and the goal is to  
58 obtain  $CO_2$  as the final product at the lowest potential and the highest current density possible.  
59 The mechanism on platinum and platinum-based catalysts comprises the occurrence of parallel  
60 pathways and involves adsorbed carbonaceous residues ( $CO_{ad}$ ,  $HCO_{ad}$ ,  $HCOO_{ad}$ , and  $COH_{ad}$ )  
61 and soluble intermediates ( $HCOOH$  and  $HCHO$ ).<sup>1-4</sup>

62 The electro-oxidation of methanol on smooth platinum is known to strongly depend on the  
63 surface structure.<sup>6</sup> Wang *et al.*<sup>7</sup> compared the electroactivity on polycrystalline platinum,  $Pt_{poly}$ ,  
64  $Pt(111)$ , and  $Pt(332)$  surfaces and observed the increase of reaction rates with increasing step  
65 sites without an appreciable increase of the  $CO_2$  production, and concluded that the defect sites  
66 enhance both parallel pathways of methanol oxidation. Shin and Korzeniewski<sup>8</sup> stated that an  
67 increase in the step density favors the methanol decomposition and the  $CO$  formation is inhibited  
68 on  $Pt(111)$  in the hydrogen adsorption potential region.

69 Housmans and Koper<sup>9</sup> through cyclic voltammetry and chronoamperometry studied the  
70 influence of stepped surfaces having (111) terraces and (110) step sites toward methanol  
71 oxidation. The authors reported that the overall oxidation rate increases with an increasing step  
72 density and that the products generated, or even methanol, can be adsorbed preferentially on step  
73 sites. Also,  $CO_{ad}$  formation is favored on step sites and its depletion is high at potentials above  
74 0.55 V vs. RHE, while methanol decomposition occurs faster than  $CO_{ad}$  oxidation at low  
75 potentials.

76 Grozovski *et al.*<sup>10</sup> reported that using (111) and (100) steps sites with (100) and (111)  
77 terraces respectively, there is no increase in the current, whereas (110) steps contribute to a  
78 higher electroactivity of methanol reaction. Also, the authors suggest that for the first step occurs  
79 a dehydrogenation, which is considered a rate-determining step because of the slowest rate in the  
80 process. Also, the effect of the anions in the oxidation process is studied. Kamyabi *et al.*<sup>11</sup>  
81 provided a detailed study on the interfacial structure on the electro-oxidation of methanol Pt  
82 single crystals.

83 Nonlinearities in electrochemical systems in the form of multi-stability and oscillating

84 reaction rates occur in many fuel cell relevant systems.<sup>12</sup> As in the case of small organic  
85 molecules<sup>12-16</sup> the electro-oxidation of methanol on platinum and platinum-based surfaces, is  
86 known for a long time to display oscillatory behavior under potentiostatic and galvanostatic  
87 regimes.<sup>17-28</sup> In general terms, electrocatalytic oscillations result from the self-organized changes  
88 in the coverage of different adsorbates, such as carbon monoxide, electrosorbing anions, and  
89 oxygenated species, for instance. The understanding of the effect of the surface structure on the  
90 kinetic instabilities is very intricate and it is still in its infancy, see ref.<sup>29</sup> and references therein.

91 We have recently investigated the effect of very tiny random surface defects on the  
92 potential oscillations along the electro-oxidation of formic on platinum.<sup>30</sup> We worked with  
93 Pt(100) electrodes disturbed by very delicate surface oxidation to different extents. As the main  
94 conclusion, it was observed that self-organized potential oscillations are much more sensitive to  
95 the surface fine structure than conventional electrochemical signatures. In particular, we proved  
96 that evolving oscillatory patterns can be employed to probe the surface fine structure *in situ* and  
97 in a non-invasive manner.<sup>30</sup> This study opened some interesting perspectives and called for  
98 further systematic investigation. The study of oscillatory reaction rates on stepped surfaces is a  
99 palpable choice in this direction.

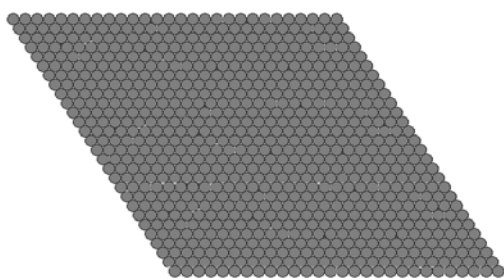
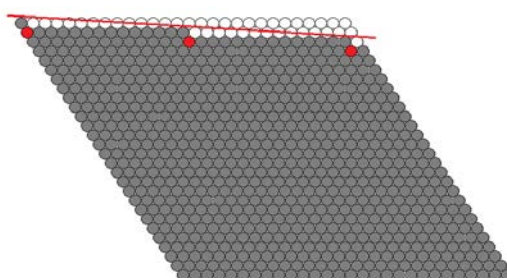
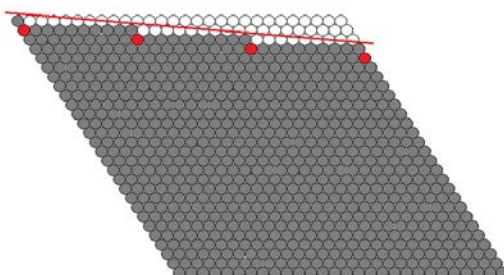
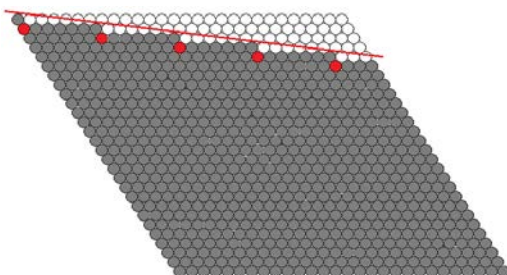
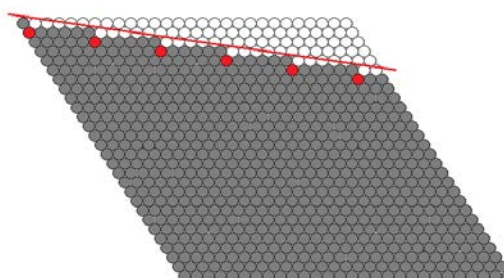
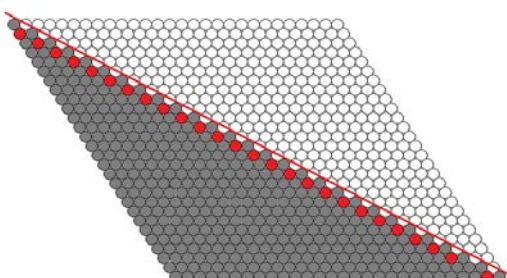
100 In the present work, we studied the electro-oxidation of methanol in acidic media on six  
101 well-defined surfaces: the basal planes Pt(111) and Pt(110) and the stepped surfaces combining  
102 these limiting orientations Pt(776), Pt(554), Pt(775), Pt(332), with focus on the oscillatory  
103 behavior under galvanostatic control. The electrodes were initially characterized and evaluated  
104 towards the electro-oxidation of methanol by means of cyclic voltammetry at two concentrations  
105 of methanol. After that, the dynamics were studied for each surface. A general discussion was  
106 provided and then the main aspects summarized.

107

## 108 **2. Experimental**

109 All platinum electrodes, low and high Miller index, used in this work were cut and  
110 polished from small single crystal platinum beads following the procedure described by Clavilier  
111 and co-workers.<sup>31</sup> The stepped surfaces, Pt(776), Pt(554), Pt(775) and Pt(332), belong to the  
112 series of Pt(S)[ $n(111) \times (111)$ ] having Miller indices Pt( $n, n, n - 2$ ). As usual,  $n$  represents the  
113 number of terrace atoms, which implies that these surfaces have 14, 10, 7 and 6 atom-wide  
114 terraces. Since the intersection of a (111) terrace and a (111) step also defines a (110) site these  
115 electrodes can be also described as a combination of ( $n - 1$ ) atom-wide (111) terraces and (110)  
116 monoatomic steps.

117 Figure 1 illustrates the one-dimension representation of stepped surfaces in the sequence  
118 along the Pt(111) to Pt(110) side of the stereographic triangle. This sequence is characterized by  
119 an increase in the amount of the (110) sites and a decrease in the size of the (111) terraces.  
120

**Pt(111)****Pt(776)****Pt(554)****Pt(775)****Pt(332)****Pt(110)**

121

122 **Fig. 1.** Two-dimensional representation of the Pt(111), Pt(776), Pt(554), Pt(775),  
123 Pt(332), and Pt(110) surfaces. Stepped surfaces Pt(776), Pt(554), Pt(775), and Pt(332)  
124 have (111) terraces of different widths and monoatomic (110) steps, and can be also

125 represented as<sup>32</sup> Pt(s)[13(111) × (110)], Pt(s)[9(111) × (110)], Pt(s)[6(111) × (110)],  
126 and Pt(s)[5(111) × (110)], respectively, see text for details.  
127

128 In the nomenclature introduced by Somorjai and co-workers,<sup>32</sup> stepped surfaces of Miller  
129 indexes Pt(776), Pt(554), Pt(775), and Pt(332), can be denoted as Pt[13(111) × (110)], Pt[9(111)  
130 × (110)], Pt[6(111) × (110)], and Pt(s)[5(111) × (110)], respectively. In this notation,<sup>32</sup>  $n(111)$   
131 means a terrace of (111) orientation, with  $n$  atomic rows in width, and monoatomic (110) steps.  
132 In other words, the stepped surface we studied, Pt(776), Pt(554), Pt(775), and Pt(332), have 13, 9,  
133 6, 5 atoms-wide (111) terraces, respectively.

134 Hydrogen (99.99%) was used for flame-annealing treatment and argon (99.998%) to  
135 deoxygenate the solution. Prior to each experiment, the electrodes were flame-annealed in a  
136 hydrogen flame and cooled in a reductive Ar:H<sub>2</sub> atmosphere (3: 1), after that they were  
137 transferred to the electrochemical cell under protection of a drop of deoxygenated ultra-pure  
138 water.<sup>33</sup>

139 All experiments were performed at 25 °C in a conventional three-electrode  
140 electrochemical cell. The chemicals used for solution preparations were sulfuric acid (Panreac,  
141 98%), Methanol (Sigma Aldrich, 99.9%), and ultrapure water from the Millipore system. The  
142 counter electrode was a 1 cm × 1 cm platinized Pt foil. The reference electrode was a reversible  
143 hydrogen electrode (RHE) and all potentials in this work are referred to it. The electrochemical  
144 measurements were performed with a Metrohm PGSTAT302N Potentiostat.

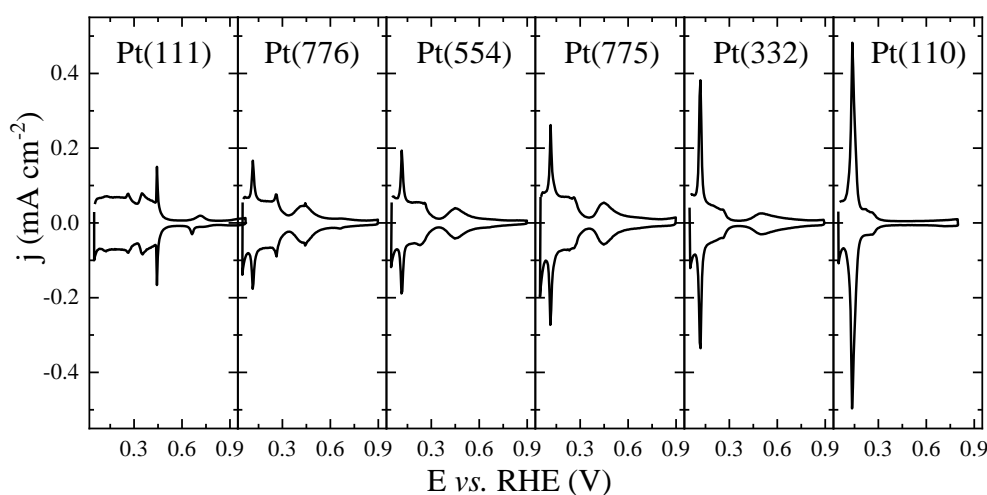
145 The platinum surface orientation and cleanliness of the electrolyte solution were checked  
146 by the stability of the characteristic cyclic voltammograms (CVs), between 0.05 and 0.80 V *vs.*  
147 RHE in a 0.5 mol L<sup>-1</sup> H<sub>2</sub>SO<sub>4</sub> aqueous solution. After that, the electrode was transferred, protected  
148 by a solution droplet, to another electrochemical cell containing a 0.5 mol L<sup>-1</sup> H<sub>2</sub>SO<sub>4</sub> and 0.2 or  
149 10.0 mol L<sup>-1</sup> MeOH solution previously deaerated with Argon (White Martins, 99.999%). Thus,  
150 to avoid changes in the electrode surface, the surfaces were always polarized at a controlled  
151 potential of 0.05 V *vs.* RHE, and the limit potential measured respecting the range between 0.05  
152 and 0.80 V *vs.* RHE. Before galvanostatic/dynamic experiments the electrodes were submitted to  
153 one voltammetric cycle in aqueous methanol solution (0.2/10 mol L<sup>-1</sup>).  
154

### 155 3. Results and Discussion

#### 156 3.1 Voltammetric characterization

157 Figure 2 shows the voltammetric profiles for all surfaces studied in this work in sulfuric  
158 acid aqueous electrolyte. These results are very similar to previously published data<sup>34,35</sup> and the

159 main characteristics observed along the sequence: Pt(111), Pt(776), Pt(554), Pt(775), Pt(332), and  
 160 Pt(110), is the decrease in the (111) domains, i.e. the featureless structure between  $\sim 0.05$  and  $0.30$   
 161 V, and the increase of the peak at (110) sites near terrace borders at  $0.13$  V. Within the hydrogen  
 162 adsorption region, that is between  $0.06$  and  $0.35$  V, the sharp peak at  $0.13$  V corresponds to  
 163 hydrogen adsorption on the 110 step sites, whereas adsorption on the terrace sites gives a broad  
 164 and featureless signal between  $0.06$  and  $0.35$  V. In the (bi)sulfate region, between  $0.35$  and  $0.8$  V,  
 165 the signal reflects the adsorption of the anion on the terrace sites.<sup>34</sup> Also, a small {100} defects  
 166 formation cannot be discarded for stepped surfaces, once a contribution at  $0.28$  V assigned to this  
 167 face is clearly seen, it is more pronounced for Pt(776) surfaces, while for the others ones are  
 168 practically unobserved.<sup>36</sup>



169

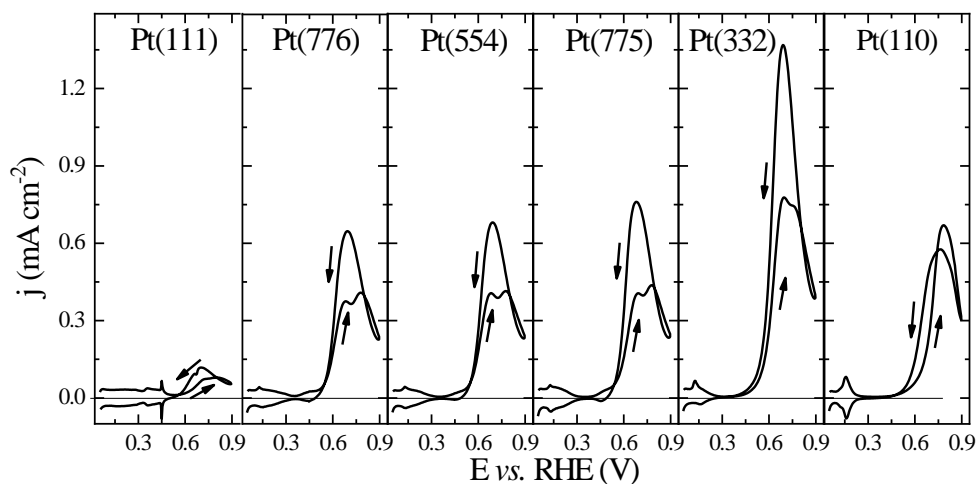
170 **Figure 2:** Cyclic voltammetry ( $v = 100 \text{ mV s}^{-1}$ ) of Pt(111), Pt(776), Pt(554), Pt(775),  
 171 Pt(332), and Pt(110) electrodes. Electrolyte: aqueous solution containing  $[\text{H}_2\text{SO}_4] =$   
 172  $0.5 \text{ mol L}^{-1}$ .  
 173

### 174 3.2 Electro-oxidation of methanol at $0.20 \text{ mol L}^{-1}$

175 The electro-oxidation of methanol on Pt stepped surfaces were investigated and the first  
 176 voltammetric cycle in each case are given in Figure 3. (FIRST SWEEP? IF SO, MAYBE IT  
 177 WOULD BE CONVENIENT TO REPORT A STATIONARY-LIKE VOLTAMMOGRAM?) –  
 178 Vinícius: after the first CV we proceed with the galvanostatic experiments, so that we do not have  
 179 subsequent cvs. The activity inferred through the voltammetric current increases in the sequence:  
 180 Pt(111) < Pt(776)  $\sim$  Pt(554)  $\sim$  Pt(775)  $\sim$  Pt(110) < Pt(332). Qualitatively, the main oxidation  
 181 wave along the positive-going sweep is split into two for the stepped surfaces, whereas a single  
 182 wave is found for Pt(111) and Pt(110). The reaction rates of the electro-oxidation of methanol

183 increase with the density of (110) sites, but small (111) terraces also contribute to the overall  
 184 process.

185



186

187 **Figure 3:** Voltammetry (at  $50 \text{ mV s}^{-1}$ ) of the electro-oxidation of methanol on  
 188 Pt(111), Pt(776), Pt(554), Pt(775), Pt(332), and Pt(110) electrodes. Electrolyte:  
 189 aqueous solution containing  $[\text{H}_3\text{COH}] = 0.20 \text{ mol L}^{-1}$  and  $[\text{H}_2\text{SO}_4] = 0.5 \text{ mol L}^{-1}$ .

190

191 On the Pt(111) electrode, anion adsorption strongly blocks the surface and the resulting  
 192 oxidation currents are very low. The hydrogen and anion adsorption processes are discernible  
 193 between 0.05 – 0.50 V; at 0.45 V the *butterfly* peak assigned to disorder-order phase transition  
 194 due to the formation of the adsorbed sulfate layer is seen. The onset potential of the electro-  
 195 oxidation of methanol starts at c.a. 0.54 V, the reverse scan showed a small hysteresis and,  
 196 thereafter, the currents fall due to the strong adsorption of sulfate anion on this surface.<sup>9</sup>

197 The hysteresis has been associated with the formation of strongly adsorbed species,  
 198 mainly CO, that are formed on the electrode surface at low potentials, during the positive-going  
 199 scan, and as the potential is scanned to high values, close to the reverse potential, these species  
 200 are oxidized. Consequently, the active sites released for further reaction show a current increase  
 201 along the negative-going sweep although shifted towards lower potentials.<sup>37</sup> This hysteresis is  
 202 observed for subsequent cycles for the oxidation of several small organic molecules.<sup>36</sup>

203 With respect to the results on the Pt(110) surface, the current peak in the hydrogen regions  
 204 is noticeable and indicates its strong adsorption, while for the stepped surfaces a small  
 205 contribution for this process is observed. The reaction currents in the positive-going scan for this  
 206 surface are relatively higher than that on most stepped surfaces, but the onset potential is

207 displaced to more positive potentials by about 100 mV. The negative-going scan is quite different  
 208 with respect to other surfaces, the peak potential is smaller than that observed in the positive  
 209 sweep.

210 Another important point to be highlighted is the influence of interfacial charge over many  
 211 electrochemical reactions, in our case, organic methanol oxidation reaction. For Pt electrodes  
 212 where several adsorption reactions occur at the same time with involving charge transference,  
 213 then the potential of zero total charge ( $E_{pztc}$ ) can be calculated measured by electrochemical  
 214 measurements and then potential of zero free charge (pzfc) was identified in different  
 215 approaches. The charge properties on the electrode surface may affect the electrocatalysis of  
 216 organic oxidation reactions, once the strongly adsorbed intermediates maybe are formed at low  
 217 potentials that maybe coincide with the PZTC zero charge potentials. CITE V. Briega-Martos, E.  
 218 Herrero, J.M. Feliu Current Opinion in Electrochemistry 2019, 17:97-105.<sup>38</sup>

219 According to Gómez *et al.*<sup>39</sup> the potential of zero total charge in aqueous sulfuric acid  
 220 shifts by 0.15 V when {110} step sites are added on (111) terraces. It appears that the pzfc of the  
 221 terrace sites shifts from the Pt(111) basal plane (0.53 V) towards positive values when the terrace  
 222 size decrease (50 and 60 mV for Pt(775) and Pt(332), respectively), while the local pzfc of the  
 223 step sites remains constant at 0.16 V, irrespectively of the terrace length. CITE R. Martinez-  
 224 Hincapie, V. Climent, J.M. Feliu, Electrochimica Acta 307 (2019) 553-563; R. Martinez-  
 225 Hincapie, V. Climent, J.M. Feliu, Current Opinion Electrochemistry 2019, 14:16-22. The authors  
 226 found<sup>39</sup> that a surface having 7 terrace-atoms, Pt(775), showed a  $E_{pzc}$  displacement of ca. 0.15 V  
 227 when compared to Pt(111) in sulfuric acid. As the conditions reported by authors were identical  
 228 to that used here, these is potentials coincides with hydrogen desorption on the terraces, while  
 229 the hydrogen desorption peak assigned to {110} monoatomic steps occurs at 0.13 V. A  
 230 comparison between Pt(111) and Pt(775) surfaces can bring us highlights about the influence of  
 231 potential of zero total charge over methanol electrocatalytic reaction. It becomes clear that  
 232 methanol oxidation takes place at potentials positive to that of zero charge.

233 In a kinetic study in pefrchloric acid invonving the series of stepped surfaces used here, it  
 234 was found that the intrinsic activity increases as the step density increases. Also, the beginning of  
 235 methanol oxidation shifted towards slightly more negative values. The surfaces were not  
 236 extremely poisoned on the {111} terraces, even in presence of {110} steps, the poison process  
 237 taking place around the pzfc of the terraces. This points out that methanol adsorbs as a neutral  
 238 molecule around the pzfc. Moreover, methanol oxidation is sensitive to anion adsorption,  
 239 pointing to a weak interaction with the electrode surface. T CITE V. Grozovski, V. Climent, E.  
 240 Herrero, J.M. Feliu, J. Electroanal. Chem. 662 (2011) 43-51 taking into account the Pt(111) and

Con formato: Inglés (Reino Unido)

Con formato: Inglés (Reino Unido)



241 Pt(775), as already was studied in the literature,<sup>39</sup> the values of  $E_{pzc}$  were 0.33 and 0.23 V,  
 242 respectively. In this respect, methanol oxidation is influenced by anion and poisoning at  
 243 potentials positive to the zero free charge. It is important to remark that sulphate anion adsorption  
 244 is particularly important on the Pt(111) basal planes, the presence of steps breaking the required  
 245 long range order to develop the widely reported ( $\sqrt{3} \times \sqrt{7}$ ) sulphate adlayer.  
 246 CITE Grozovski and reference 9 from Marc Koper. According to Fig. 2 is possible to compare the  
 247 CVs of methanol electrooxidation, an analysis of Pt(111) reveals that the  $E_{pzc}$  occurs close to  
 248 hydrogen region, therefore no relevant contribution to form intermediates like CO is observed for  
 249 this surface at this potential, once the surface charge is composed mostly by anions. [xx] In  
 250 addition, the low rate methanol reaction lies in the strong anion adsorption, which below of 0.45  
 251 V, (bi)sulfate starts to desorb from the Pt(111), consequently, the active sites are unavailable to  
 252 further methanol adsorption.<sup>9</sup>

253 Now, considering a Pt(332), that it was the most active surface in our study, and  
 254 comparing it with the stepped surface studied by Gómez and co-workers,<sup>39</sup> the addition of step  
 255 sites shifts the  $E_{pzc}$  to more negative potentials compared to Pt(111). Differently to the latter  
 256 surface, the potential of zero total charge is ca. at 0.23 V,<sup>39</sup> where the anion is present on the  
 257 terrace. Thereafter this potential the currents registered in the CV increases significantly, this  
 258 implies that methanol oxidation is strongly catalyzed by the presence of step sites that further  
 259 contribute to diminishing the anion adsorption. However, the interfacial surface charge for  
 260 stepped surface seems to be formed by species highly active, this assumption is supported by  
 261 Koper *et al.*<sup>9</sup> where (111) terraces lead to an improvement over the reaction rate, probably as a  
 262 result of disruption of the anion adlayer. Summarizing In summary, the electro-oxidation of  
 263 methanol strongly depends on the surface arrangement, we have observed that and {110} steps  
 264 sites influences positively the electro-oxidation of methanol. However,, once these stepped  
 265 surfaces are more susceptible in forming CO at low potentials due to different adsorption of water  
 266 and electrolyte anions, that play an important rule role over the electroactivity for MEO.<sup>9,10</sup>

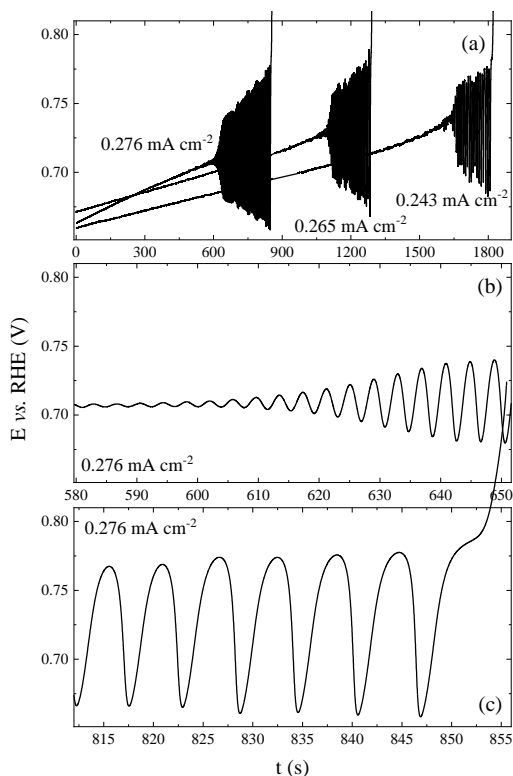
267 The system was investigated under galvanostatic regime and the potential oscillations were  
 268 nearly unaffected by the electrode surface at  $[H_3COH] = 0.20 \text{ mol L}^{-1}$ . This is somehow  
 269 surprising given the differences observed in the voltammetric profiles. Figure 4 illustrates  
 270 representative oscillations for the Pt(554) surface. The effect of the applied current is given in  
 271 panel 4(a); harmonic oscillations observed near the onset and slightly higher amplitude are  
 272 presented in Figure 4(b) and (c), respectively. The oscillatory frequencies near the bifurcation  
 273 point generally increase with the applied current for a given surface and range from 0.10 to 0.50  
 274 Hz in all cases, c.f. Figure S1 in [Supplementary File](#). These small amplitude oscillations are

Código de campo cambiado

Con formato: Sangría: Primera línea:  
0 cm, No ajustar espacio entre texto  
latino y asiático

275 slower than those found on Pt<sub>poly</sub>.<sup>22,23</sup> As already reported,<sup>29</sup> no oscillations were observed on the  
 276 as-prepared Pt(111) surface.

277



278

279 **Figure 4:** Oscillatory electro-oxidation of methanol on Pt(554) (a) at three applied  
 280 currents. Details of oscillations at 0.276 mA cm<sup>-2</sup>, are given in (b) and (c).  
 281 Electrolyte: aqueous solution containing [H<sub>3</sub>COH] = 0.20 mol L<sup>-1</sup> and [H<sub>2</sub>SO<sub>4</sub>] = 0.5  
 282 mol L<sup>-1</sup>.  
 283

284 After this initial assessment, we looked for parameter regions where the effect of surface  
 285 sites becomes more pronounced. It is already known that potential oscillations along the electro-  
 286 oxidation of methanol on platinum are mainly encountered in two modes:<sup>17,18,21–23,25–27</sup> small  
 287 amplitude and high frequency, type *S*, and large amplitude and low frequency, type *L*.  
 288 Oscillations of type *L* are often associated to mixed-mode oscillations with the superposition of  
 289 small modulations at high potentials.<sup>25</sup> The occurrence of both types *S* and *L* and also the number  
 290 of potential modulations present in the later have been used to characterize very tiny surface  
 291 structures.<sup>30</sup>

292 Okamoto and co-workers<sup>40</sup> reported a detailed study of the experimental parameters  
293 where oscillations of type *S* and *L* are found. Overall, the occurrence of both oscillations  
294 separated by a quiescent period is favored at high methanol concentration. Based on this work,  
295 we decided to carry out experiments with  $[\text{H}_3\text{COH}] = 10 \text{ mol L}^{-1}$ , where separated *S* and *L*  
296 windows, and thus mixed-mode oscillations, are expected to occur abundantly.<sup>40</sup>

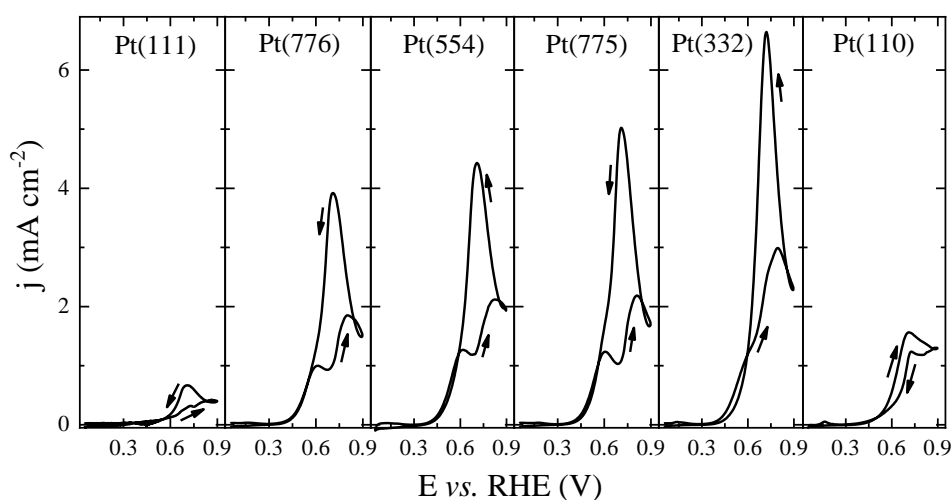
297

### 298 **3.3 Electro-oxidation of methanol at 10 mol L<sup>-1</sup>**

299 Figure 5 depicts the voltammetric profiles for the electro-oxidation of methanol at 10 mol  
300 L<sup>-1</sup>. The two limiting surfaces, corresponding to the basal planes, show the lower activities, with  
301 Pt(110) being considerably more active than Pt(111). The voltammetric signatures of the electro-  
302 oxidation of methanol on stepped electrodes reinforce the pivotal role of surface structure. The  
303 two current peaks are again found here, at about 0.60 and 0.80 V and more pronounced than that  
304 for  $[\text{H}_2\text{SO}_4] = 0.20 \text{ mol L}^{-1}$ . The first peak is somewhat suppressed on Pt(332), the 6-atoms  
305 terrace surface.

306 The activities of the stepped surfaces follow the trend observed for  $[\text{H}_3\text{COH}] = 0.20 \text{ mol}$   
307 L<sup>-1</sup> but with more pronounced differences in the voltammetric currents: Pt(776) < Pt(554) <  
308 Pt(775) < Pt(332). Again, the increase in the density of (110) sites clearly increases the reaction  
309 rates for the electro-oxidation of methanol, but small (111) terraces also contribute to the overall  
310 process. For the sake of comparison, the activity on polycrystalline platinum at this high  
311 concentration, as inferred from the current maximum in the cyclic voltammogram, is slightly  
312 smaller (Figure S2) than that found for the Pt(332) electrode, yet larger than that for Pt(775),  
313 Figure 5.

314



315

316 **Figure 5:** Voltammetry (at  $50 \text{ mV s}^{-1}$ ) of the electro-oxidation of methanol on  
 317 Pt(111), Pt(776), Pt(554), Pt(775), Pt(332), and Pt(110) electrodes. Electrolyte:  
 318 aqueous solution containing  $[\text{H}_3\text{COH}] = 10 \text{ mol L}^{-1}$  and  $[\text{H}_2\text{SO}_4] = 0.5 \text{ mol L}^{-1}$ .  
 319

320 Another interesting point is concerning to the hysteresis effect observed for all stepped  
 321 surfaces, the same behavior is not observed for Pt(110), the currents in the negative-going scan  
 322 were lower than those presented in the anodic profile and a peak at 0.73 V appears. Herein the  
 323 species strongly adsorbed formed during the positive-going scan, specially at high potentials,  
 324 seems to keep on the surface without being oxidized, once no free Pt sites are available to  
 325 proceed with the reaction and, thus, the hysteresis is inhibited.

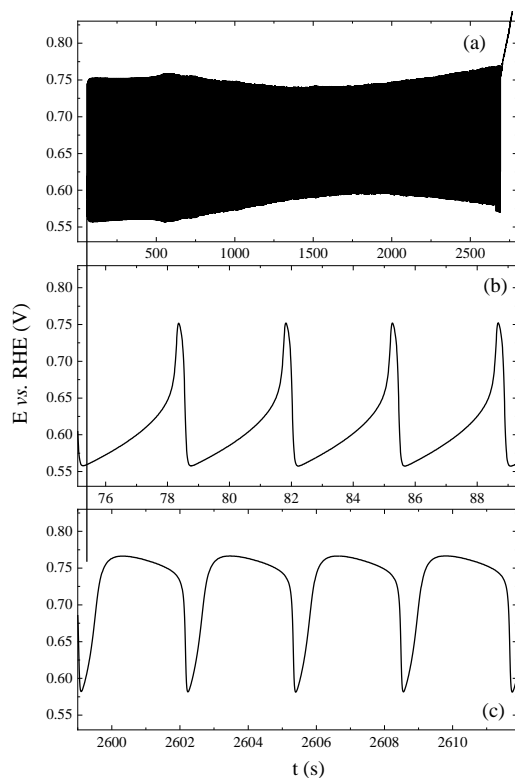
326 After the voltammetric characterization, we proceeded with a detailed study of the electro-  
 327 oxidation of methanol under galvanostatic conditions and no oscillations were found on Pt(111)  
 328 and Pt(110), the less active surfaces according to Figure 5. In contrast to that observed for  
 329  $[\text{H}_3\text{COH}] = 0.20 \text{ mol L}^{-1}$ , the surface structure of the stepped surfaces clearly influences the  
 330 resulting dynamics. In the following, we discuss the peculiarities in the potential oscillations  
 331 according to the stepped surface.

332

### 333 **Dynamics on Pt(776), Pt(s)[13(111) × (110)], electrode.**

334 Potential oscillations along the electro-oxidation of methanol on Pt(776) were studied at  
 335 different applied currents (from 0.492 to  $1.60 \text{ mA cm}^{-2}$ ), results are given in Figure S3 in the  
 336 **Supplementary File**. Overall, the duration of the oscillations decreases with the increase of the  
 337 applied current.<sup>25,41,42</sup> Typical oscillations are illustrated in Figure 6 for an applied current of  
 338  $0.738 \text{ mA cm}^{-2}$  and in terms of the (a) overall time-series, (b) initial, and (c) final cycles.

339 Generally speaking, the oscillatory features given in Figure 6 resemble those observed in  
 340 polycrystalline platinum, even at different temperatures,<sup>23</sup> but interesting dissimilarities are also  
 341 present. For comparison, Figure S4 in the [Supplementary File](#) shows typical potential oscillations  
 342 for the electro-oxidation of methanol at this unusual high concentration ( $10 \text{ mol L}^{-1}$ ) on  $\text{Pt}_{\text{poly}}$ .  
 343



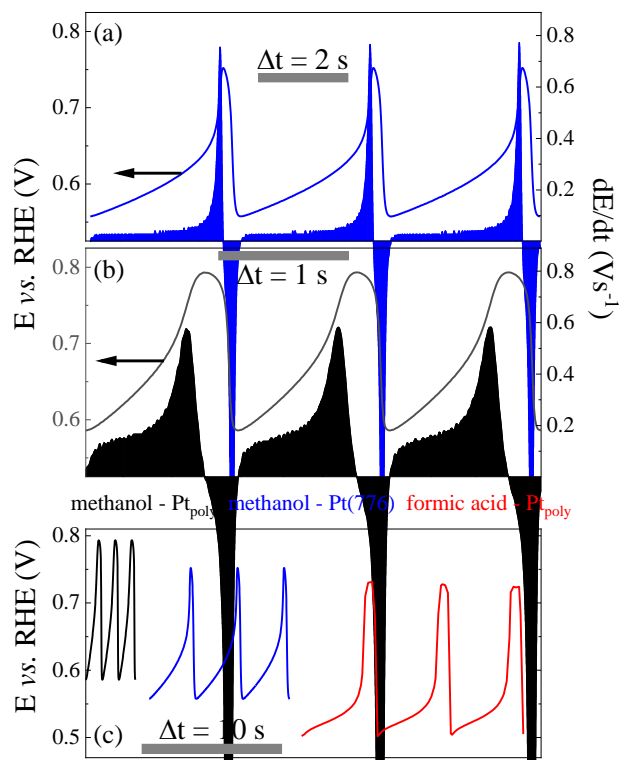
344

345 **Figure 6:** Oscillations in the electro-oxidation of methanol on a Pt(776) electrode, at  
 346  $0.738 \text{ mA cm}^{-2}$ . Electrolyte: aqueous solution containing  $[\text{H}_3\text{COH}] = 10 \text{ mol L}^{-1}$  and  
 347  $[\text{H}_2\text{SO}_4] = 0.5 \text{ mol L}^{-1}$ .  
 348

349 Figure 7 exhibits the contrast of the initial, relaxation-like, oscillations on (a) Pt(776) and  
 350 (b)  $\text{Pt}_{\text{poly}}$ , in terms of time-series and their time-derivative. Oscillations on Pt(776) have an  
 351 amplitude of  $\sim 200 \text{ mV}$  ( $0.55 - 0.75 \text{ V}$ ), and a period of  $3.5 \text{ s}$ ; on  $\text{Pt}_{\text{poly}}$  oscillations occur between  
 352  $0.60$  and  $0.78 \text{ V}$ , and are faster, with a period of  $1.2 \text{ s}$ . In terms of the oscillations' waveform, less  
 353 round, steeper oscillations characterize the dynamics on Pt(776), when compared to that on  $\text{Pt}_{\text{poly}}$ .  
 354 The  $dE/dt$  profiles<sup>43</sup> given in panels (a) and (b) further evidence that the oscillations on Pt(776)

355 surface have a more well-defined two poisoning processes; in contrast, the  $dE/dt$  evolution on  
 356  $Pt_{poly}$  is clearly smoother.

357



358

359 **Figure 7:** Time-series (and their time-derivative) of the oscillatory electro-oxidation  
 360 of methanol on (a) Pt(776), at  $0.738 \text{ mA cm}^{-2}$ , and (b) on  $Pt_{poly}$ , at  $1.445 \text{ mA cm}^{-2}$ .  
 361 Electrolyte: aqueous solution containing  $[\text{H}_3\text{COH}] = 10 \text{ mol L}^{-1}$  and  $[\text{H}_2\text{SO}_4] = 0.5$   
 362  $\text{mol L}^{-1}$ . (c) the same time-series as in (a) and (b), and also for the electro-oxidation of  
 363 formic acid on  $Pt_{poly}$ , for sake of comparison, taken from Figure 2(b) at  $0.88 \text{ mA cm}^{-2}$   
 364 in reference <sup>43</sup>.

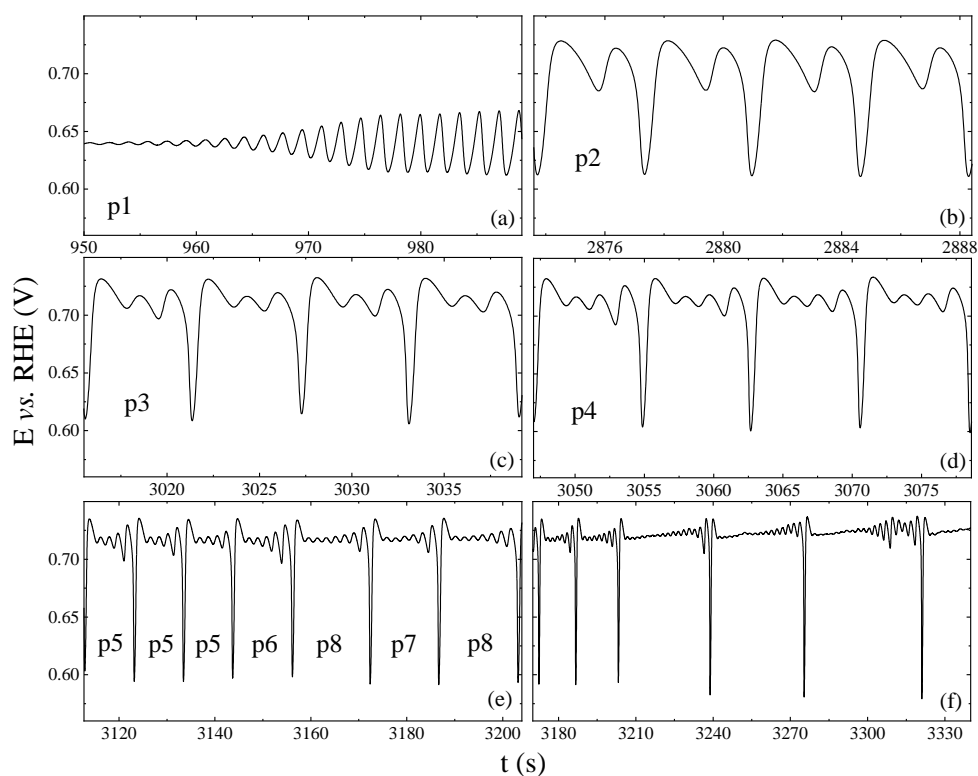
365

366 Figure 7(c) also includes typical oscillations recorded for the oscillatory electro-oxidation  
 367 of formic acid on  $Pt_{poly}$  <sup>43</sup> in addition to the comparison between methanol on Pt(776) and  $Pt_{poly}$ .  
 368 From left to right, in the sequence: methanol on Pt(776) – methanol on  $Pt_{poly}$  – formic acid on  
 369  $Pt_{poly}$ , it becomes apparent that the active state, i.e. the lower potential limit, decreases; the  
 370 frequency decreases; and the oscillations get steeper; besides the features already mentioned.  
 371 Therefore, it becomes clear that oscillations during the electro-oxidation of methanol on Pt(776)  
 372 somewhat resemble those found for the electro-oxidation of formic acid on  $Pt_{poly}$ . <sup>43</sup> In terms of

373 reaction mechanism, a remarkable difference between potential oscillations found in the electro-  
374 oxidation of methanol and formic acid on Pt<sub>poly</sub> is the larger variation in the coverage of adsorbed  
375 CO,  $\theta_{CO}$ , in the case of the later.<sup>26</sup> In fact, the amplitude of oscillations in  $\theta_{CO}$  has been  
376 investigated by means of *in situ* infrared (IR) spectroscopy in the attenuated total reflection  
377 (ATR) configuration using a platinum film, and it was found to range from 0.24 to 0.37 ML,<sup>26</sup>  
378 and from 0.20 to 0.40 ML,<sup>44</sup> for the electro-oxidation of methanol and formic acid on Pt<sub>poly</sub>,  
379 respectively. Therefore, the features described for the oscillations on Pt(776) can be thought of a  
380 result of the larger amplitude of the oscillating coverage of adsorbed CO, and thus of the higher  
381 activity of the surface. A decisive proof of this argument is in principle unfeasible because of the  
382 impossibility of doing experiments with stepped surfaces using the ATR configuration.  
383 Nevertheless, this inference is fully supported by experiments with stepped surfaces, where the  
384 amount of adsorbed CO increases with the increase of density of step sites.<sup>9</sup> This is an intrinsic  
385 feature, and the steeper waveforms with a more discernible definition of two regions of  
386 poisoning, c.f. Figure 7(a), characterize the potential oscillations found in all stepped surfaces  
387 investigated here.

388 Figure 8 shows the time evolution of the oscillatory electro-oxidation of methanol on  
389 Pt(776) at 0.492 mA cm<sup>-2</sup>. As in the case found on Pt<sub>poly</sub>,<sup>22</sup> oscillations set in via a supercritical  
390 Hopf bifurcation with sinusoidal waveform and develop in time, analogously to that observed  
391 when the applied current is increased,<sup>25,41</sup> to chaotic behavior. Mixed-mode oscillations are  
392 usually registered in between,<sup>25</sup> with the intercalation of *one* large and *n* small amplitude  
393 oscillations,  $LS^n$ . The total period (n+1) computed for the time evolution in Figure 8 clearly  
394 denotes a period-adding sequence from 1 to 6, with periods 7 and 8 being also detected. The  
395 accumulation of small modulations at high potentials become hard to distinguish and eventually  
396 gives rise to chaos; nevertheless, periods 7 and 8 are also observed after period 6.

397



398

399 **Figure 8:** Time evolution of the oscillatory electro-oxidation of methanol on a  
 400 Pt(776) electrode at  $0.492 \text{ mA cm}^{-2}$ . Electrolyte: aqueous solution containing  
 401  $[\text{H}_3\text{COH}] = 10 \text{ mol L}^{-1}$  and  $[\text{H}_2\text{SO}_4] = 0.5 \text{ mol L}^{-1}$ .

402

403 The emergence of these mixed-mode states obviously depends on parameters such as  
 404 applied current, but since all surfaces were investigated under comparable conditions, it is clear  
 405 that the observed systematized period-adding sequence is favored on Pt(776) surfaces. It is thus  
 406 plausible to infer that this specific configuration stabilizes the modulation around high potentials.  
 407 This observation is in line with the presence of this type of mixed-mode oscillations on  $\text{Pt}_{\text{poly}}$ ,  
 408 which contains a considerable amount of (111) terraces. Indeed, comparable period-adding  
 409 sequences for the electro-oxidation of methanol have been also observed on  $\text{Pt}_{\text{poly}}$ .<sup>18,22,25,40</sup> For  
 410 instance, Okamoto and co-workers described similar oscillations with transitions from 1 to 3,<sup>40</sup>  
 411 and from 1 to 5,<sup>18</sup> but with some irregularities in between. Furthermore, if the (111) promotes the  
 412 development of those small modulations, additional sites are also needed for oscillations, as they  
 413 are apparently absent on Pt(111) electrodes.<sup>29</sup>

414



415 ***Dynamics on Pt(554), Pt(s)[9(111) × (110)], electrode.***

416 Oscillatory behavior on this surface was rather similar to that on Pt(776), but with less  
417 complete sequence of period-adding patterns. Oscillations were found from 0.5 to 0.72 mA cm<sup>-2</sup>  
418 and typical data are presented in Figure S5 in the [Supplementary File](#) for intermediate applied  
419 current. Again, oscillations presented in Figure S5(b) clearly show the steep transition to high  
420 potentials discussed above, c.f. Figure 6(b).

421

422 ***Dynamics on Pt(775), Pt(s)[6(111) × (110)], electrode.***

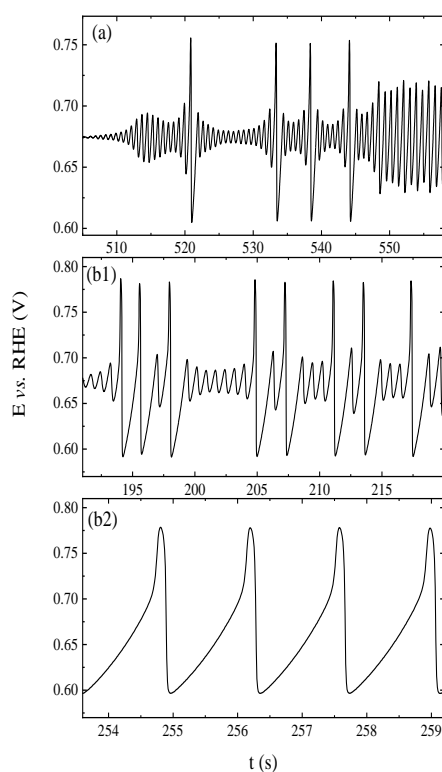
423 Typical oscillations on this surface are given in the [Supplementary File](#), Figure S6. Most  
424 features discussed above are also preserved here. The prevalence of steeper oscillations also  
425 occurs on this surface, Figure S6(b), reinforcing thus the observation that this specific feature of  
426 stepped surfaces. As illustrated in Figure S6 (a1) and in detail in (a2), there is a *quiescent period*  
427 *between small amplitude oscillations*. The appearance of such a quiescent period, previously  
428 unreported, is somewhat common in the potential oscillations along the electro-oxidation of  
429 methanol, but it seems that only slower and larger amplitude oscillations have been observed  
430 after this dormant interval.<sup>17</sup> This is confirmed in the systematic work performed by Mukouyama  
431 *et al.*<sup>40</sup> The occurrence of this quiescent interval between small amplitude oscillations depends on  
432 the applied current and at slightly higher currents on, oscillations change to high amplitude ones  
433 quickly, c.f. Figure S6(b).

434

435 ***Dynamics on Pt(332), Pt(s)[5(111) × (110)], electrode.***

436 Figure 9 shows snapshots of two time-series, @1.445 and 1.735 mA cm<sup>-2</sup>, recorded on  
437 Pt(332), the surface with the smallest (111) terraces studied (n = 5). Intricate high frequency, low  
438 amplitude, stiff oscillations are observed around the bifurcation point in (a). At higher currents,  
439 c.f. panel (b1), these oscillations are clearly discernible. Qualitatively, the small modulations that  
440 co-exist with the higher amplitude oscillations occur in a potential region placed *around the mean*  
441 *value of the high amplitude oscillations*. In contrast, mixed-mode and chaotic potential  
442 oscillations along the electro-oxidation of methanol on platinum<sup>18</sup> are mainly characterized by the  
443 presence of small amplitude modulations *around the upper potential limit*. The irregular/chaotic  
444 oscillations found on Pt(332) are somewhat faster than those on Pt<sub>poly</sub>. The estimated frequencies  
445 for the large amplitude oscillations in Figure 9(b1) vary from about 0.1 to 0.5 Hz, whereas the  
446 ones on Pt<sub>poly</sub> fall into the range 0.025 – 0.05 Hz, as illustrated in Figure 8(f). The conventional  
447 modulations at high potentials, c.f. Figure 8(f), occurs after the decrease of the electrode potential  
448 after reaching this maximum. In contrast, small amplitude modulations on the Pt(332) electrode

449 emerge after the increase of the potential from its lower limit, i.e. the most active state. The  
 450 potentials visited in the course of the self-organized oscillations reflect the nature and coverage of  
 451 adsorbed species so that the peculiar oscillations found on Pt(332) are certainly associated with  
 452 different surface chemistry reactivity than that on Pt<sub>poly</sub>.



453

454 **Figure 9:** Oscillatory electro-oxidation of methanol on Pt(332) surface, at different  
 455 applied currents: (a) 1.445 mA cm<sup>-2</sup>, and (b) 1.735 mA cm<sup>-2</sup>. Electrolyte: aqueous  
 456 solution containing [H<sub>3</sub>COH] = 10 mol L<sup>-1</sup> and [H<sub>2</sub>SO<sub>4</sub>] = 0.5 mol L<sup>-1</sup>.  
 457

458 Oscillations illustrated in Figure 9(b1) have apparently no parallel in the electro-oxidation  
 459 of methanol on platinum under comparable conditions. Sitta and co-workers<sup>45</sup> reported the  
 460 presence of small modulations around the mean value for this system but at pH 2.15. The general  
 461 waveforms of these oscillations are unlike those reported here and are probably due to the  
 462 relatively higher pH used. This specific type of chaotic dynamics exemplified in Figure 9(b1) was  
 463 observed here only on Pt(332), the surface with the smallest (111) terraces studied. This  
 464 observation on this limiting stepped surface can be thought as an evolution of the stiffer  
 465 oscillations present in stepped surfaces. **HAVE WE DATA WITH SURFACES WITH**  
 466 **SHORTEST TERRACES? – unfortunately we don't.**

467

468 **3.4 General discussion**

469 Comparing the oscillatory electro-oxidation of methanol on polycrystalline and on single  
470 crystal and stepped surfaces can be very illustrative. Dynamics on Pt(111), Pt(100), and Pt(100)  
471 surfaces have been reported.<sup>29</sup> In the present work we present and discuss the experimental  
472 investigation of the oscillatory electro-oxidation of methanol on stepped platinum electrodes,  
473 namely surfaces with (111) terraces of different sizes and monoatomic (110) steps: Pt(776),  
474 Pt(554), Pt(775), and Pt(332), besides Pt(111) and Pt(110). The voltammetric activity on stepped  
475 surfaces was generally higher than that on Pt(111) and Pt(110). Importantly, more than simply a  
476 matter of activity, the spontaneous emergence of potential oscillations revealed peculiar,  
477 previously unseen, aspects of the stepped surfaces.

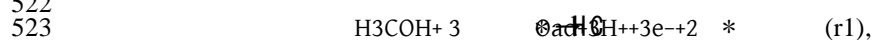
478 Oscillations at lower methanol concentrations ( $0.20 \text{ mol L}^{-1}$ ) were nearly independent on  
479 the surface structure and only small amplitude oscillations were recorded. Previous studies<sup>30</sup>  
480 indicated that the concomitant presence of oscillations of small, *S*, and large, *L*, amplitudes can be  
481 useful to distinguish very small differences in surface structure. Okamoto and co-workers<sup>40</sup> found  
482 that higher methanol concentrations promote the appearance of *S* and *L* oscillations. Therefore,  
483 we performed experiments at  $[\text{H}_3\text{COH}] = 10 \text{ mol L}^{-1}$ , and, indeed, very interesting behavior was  
484 registered. Alternatively to the enhancement of the mass transport conditions, using, for instance,  
485 a rotating disk electrode, increasing the bulk concentration of methanol enhances its  
486 concentration in the neighborhood of the electrode, but do not promote the removal of partially  
487 oxidized species from the electrode vicinity.<sup>7,46-48</sup> In fact, we have shown that oscillations of type  
488 *L* are suppressed when the solution is stirred.<sup>30</sup> Possible candidates of partially oxidized species  
489 that could play a role in the generation of *L* oscillations are dissolved  $\text{HCOOCH}_3$ ,  $\text{HCOOH}$ , and  
490  $\text{HCHO}$  species.

491 The main characteristics of the galvanostatic oscillations recorded on the stepped surfaces  
492 are the steep transition to high potentials, higher amplitudes, lower frequencies and also the lower  
493 potentials reached, c.f. Figure 7(c). These features prevail in all stepped surfaces studied and  
494 reflect the simultaneous presence of (111) terraces separated by monoatomic (110) steps.  
495 Mechanistically speaking, the comparison among the potential oscillations in the electro-  
496 oxidation of methanol on  $\text{Pt}_{\text{poly}}$  and on stepped Pt surfaces, and in the electro-oxidation of formic  
497 acid on  $\text{Pt}_{\text{poly}}$  suggests that the oscillatory behavior and the correspondingly higher voltammetric  
498 activities on stepped surfaces are probably also related to the higher amplitude in the CO  
499 coverage along the process. In addition, the shape of the potential increase depicted in Figure 7  
500 indicates a more complex, two-step, poisoning process. On disordered polycrystalline surfaces,

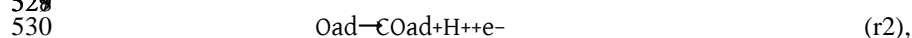
501 the poisoning process is usually smoother and more subtle and delicate processes are apparently  
 502 hidden, likely because the lack of surface structure control.

503 Further analysis of the oscillatory dynamics on stepped surfaces reinforces the  
 504 peculiarities associated with the specific sizes of the (111) terraces. In contrast to the trivial trends  
 505 in the voltammetric signatures, very reproducible and specific features were found under  
 506 oscillatory regime. Large (111) domains, on Pt[13(111) × (110)], Pt(776) electrode, were found  
 507 to stabilize the small amplitude modulations found around the upper potential limit in *L*-type  
 508 oscillations, resulting in an unparallel complete period-adding sequence of mixed-mode  
 509 oscillations. On Pt(775), the 6 atoms-wide (111) terraces surfaces, a peculiar separation between  
 510 oscillations of *S*-type was observed at low applied currents. Finally, a new type of potential  
 511 oscillations for the electro-oxidation of methanol was found for the limiting surface studied: the  
 512 stepped surface with smaller, only five atoms wide, (111) terraces studied, the Pt(s)[5(111) ×  
 513 (110)] ≡ Pt(332) surface. These oscillations resemble the steep features mentioned for the stepped  
 514 surfaces but develop into mixed-mode oscillations completely distinct from that previously  
 515 observed for this system. Whereas modulations around high potentials values usually found in  
 516 conventional mixed-mode oscillations in this system are due to the difficulty to completely  
 517 oxidize the adsorbed carbon monoxide, modulations around intermediate values found here on  
 518 Pt(332), certainly reflect a different mechanistic origin.

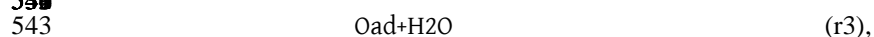
519 We have discussed some mechanistic aspects of the oscillatory electro-oxidation of  
 520 methanol on polycrystalline platinum.<sup>24,30</sup> Herein we summarize some critical aspects relevant to  
 521 the present discussion. Site-demanding steps, including for instance methanol dehydrogenation,



524 are likely to require terraces and are thus influenced by the size of (111) domains. Herein \*  
 525 accounts for a free platinum site. On the other hand, monoatomic (110) steps, as well as defect  
 526 sites, are expected to favor the formation of adsorbed carbon monoxide,<sup>9</sup> either from  $\text{HCO}_{\text{ad}}$ :



531 or via the re-adsorption of the mentioned partially oxidized species:



544 and,



557 Partially oxidized species, viz.  $\text{HCOOCH}_3$ ,  $\text{HCOOH}$ , and  $\text{HCHO}$ , are expected to play a role in  
 558 the oscillations observed here.<sup>30</sup>

559 In addition, the formation of oxygenated species from water,<sup>49,50</sup> is also privileged on step  
 560 sites. The presence of such species is critical to the Langmuir-Hinshelwood step:



562  
 563  
 564 Steps r1-5 include clearly non-elementary, cf. (r1), and, presumably, elementary steps,  
 565 (r2) for instance. Besides the simplified picture discussed along with these steps, all possible  
 566 steps depend on the surface structure. The voltammetry responses illustrated in Figures 3 and 5,  
 567 indicates that the presence of (110) steps clearly enhances the oxidation rates, but the activity  
 568 decreases on Pt(110) electrode, unambiguously attesting that terraces of (111) orientation are also  
 569 needed to reach high rates. The oscillatory dynamics found here clearly points to a more intricate  
 570 dependence on the surface structure. Solving the whole puzzle, however, is an ongoing task, and  
 571 further studies, preferentially combining experiments, modeling, and simulations, are in progress.  
 572 Importantly, this study further reinforces the importance of electrochemical oscillations in  
 573 electrocatalysis,<sup>12,16</sup> mainly by revealing relevant features that are hidden under regular, non-  
 574 oscillatory conditions.

575

#### 576 4. Conclusions

577 We reported in this paper results of the electro-oxidation of methanol on stepped  
 578 Pt[n(111) x (110)] surfaces under voltammetric and galvanostatic regime, where potential  
 579 oscillations emerge. The study was carried out in acidic media (aqueous sulfuric acid electrolyte)  
 580 and on Pt(111), Pt(110), and on stepped surfaces Pt(776), Pt(554), Pt(775), and Pt(332). It was  
 581 found that the reaction rates of the electro-oxidation of methanol increase with the density of  
 582 (110) sites, but small (111) terraces also contribute to the overall process, as the Pt(332) surface is  
 583 considerably more active than Pt(110). In particular, the electrocatalytic activity, as inferred in  
 584 the voltammetric current, was found to increase in the sequence: Pt(111) < Pt(776) ~ Pt(554) ~  
 585 Pt(775) ~ Pt(110) < Pt(332), when  $[\text{H}_3\text{COH}] = 0.20 \text{ mol L}^{-1}$ ; and: Pt(111) < Pt(110) << Pt(776) <  
 586 Pt(554) < Pt(775) < Pt(332), for  $[\text{H}_3\text{COH}] = 10 \text{ mol L}^{-1}$ .

587 Under oscillatory regime, the effect of the interfacial structure can get even more  
 588 complicated than the changes in the trends of the overall activity, as several adsorption and  
 589 reaction steps are simultaneously active during self-organized potential or current oscillations.  
 590 Indeed, the potential oscillations observed under galvanostatic control, display specificities  
 591 unambiguously assigned to the surface structure.

592 At  $[\text{H}_3\text{COH}] = 0.20 \text{ mol L}^{-1}$  no oscillations were found on Pt(111), and only small  
 593 amplitude (S-type) oscillations were observed for other surfaces, with oscillatory frequencies

594 between 0.10 and 0.50 Hz. At  $[H_3COH] = 10 \text{ mol L}^{-1}$  no oscillations were observed on the  
595 limiting surfaces, i.e. Pt(111) and Pt(110). For the stepped surfaces, the size of the (111) terraces  
596 and density of step sites were found to clearly affect the oscillatory dynamics. First of all, the  
597 large amplitude, relaxation-like oscillations found on stepped surfaces are clearly different than  
598 those found on polycrystalline platinum,  $Pt_{poly}$ . Taking the Pt(776) as a representative example,  
599 potential oscillations have an amplitude of  $\sim 200 \text{ mV}$  (0.55 – 0.75 V), and a period of 3.5 s; on  
600  $Pt_{poly}$  oscillations under identical conditions occur between 0.60 and 0.78 V and have a period of  
601 1.2 s. Interestingly, the oscillations' waveform and less round and steeper on stepped surfaces,  
602 when compared to  $Pt_{poly}$ . The comparison of the potential oscillations in the electro-oxidation of  
603 methanol on stepped and polycrystalline surfaces with previously published data<sup>26,43,44</sup> suggested  
604 that the amplitude of the oscillating coverage of  $CO_{ad}$  is larger on stepped surfaces. This is in  
605 agreement with previous reports that attest that the amount of adsorbed CO increases with the  
606 increase of density of step sites.<sup>9</sup> This feature is present in all stepped surfaces studied and thus  
607 results of the presence of (111) terraces separated by monoatomic (110) steps. In fact, the larger  
608 amplitude of the oscillating coverage of  $CO_{ad}$  is likely to be the main mechanistic aspect  
609 underlying the dynamic features assigned to the stepped surfaces.

610 The specific features assigned to the surface structure are summarized as follows: (a) 13  
611 atoms-wide (111) domains, on  $Pt[13(111) \times (110)] \equiv Pt(776)$  electrode, stabilized the small  
612 amplitude modulations found around the upper potential limit in *L*-type oscillations, resulting in  
613 an unparallel complete period-adding sequence of mixed-mode oscillations; On the 6 atoms-wide  
614 (111) terraces, Pt(775), surfaces, a peculiar separation between oscillations of *S*-type was  
615 observed at low applied currents; A new type of potential oscillations was found on the stepped  
616 surface with smaller, only five atoms wide, (111) terraces surface studied here, i.e.  $Pt(s)[5(111) \times$   
617  $(110)] \equiv Pt(332)$ .

618 We have pursued modeling and numerical simulations of oscillatory behavior in  
619 electrocatalytic systems as a way of obtaining reliable reaction rate constants.<sup>51,52</sup> This approach  
620 uses experimental data to provide a micro-kinetic description of the whole system, rather than  
621 fitting chronoamperometric data, for instance. Experimental results using well-ordered single  
622 crystal surfaces like the ones reported here are certainly of help in the investigation of how a  
623 given surface site influences specific reaction steps.

624

## 625 **Acknowledgments**

626 GTF and HV (Grant No. 2013/16930-7) acknowledge São Paulo Research Foundation (FAPESP)  
627 for financial support. HV (Grant No. 306060/2017-5) acknowledges Conselho Nacional de  
628 Desenvolvimento Científico e Tecnológico (CNPq) for financial support. This study was partially  
629 financed by the Coordenação de Aperfeiçoamento de Pessoal de Nível Superior – Brasil  
630 (CAPES) – Finance Code 001. Authors thank Dr. B. A. F. Previdello for experimental assistance.  
631

## 632 References

- 633  
634 1 R. Parsons and T. VanderNoot, *J. Electroanal. Chem.*, 1988, **257**, 9–45.  
635 2 S. Wasmus and A. Küver, Methanol oxidation and direct methanol fuel cells: a selective  
636 review, *J. Electroanal. Chem.*, 1999, **461**, 14–31.  
637 3 T. Iwasita, Electrocatalysis of methanol oxidation, *Electrochim. Acta*, 2002, **47**, 3663–  
638 3674.  
639 4 N. M. Markovic and P. N. Ross Jr., Surface science studies of model fuel cell  
640 electrocatalysts, *Surf. Sci. Rep.*, 2002, **45**, 117–229.  
641 5 S. Sriramulu, T. D. Jarvi and E. M. Stuve, A kinetic analysis of distinct reaction pathways  
642 in methanol electrocatalysis on Pt(111), *Electrochim. Acta*, 1998, **44**, 1127–1134.  
643 6 E. Herrero, K. Franaszczuk and A. Wieckowski, Electrochemistry of methanol at low  
644 index crystal planes of platinum. An integrated voltammetric and chronoamperometric  
645 study, *J. Phys. Chem.*, 1994, **98**, 5074–5083.  
646 7 H. Wang and H. Baltruschat, DEMS study on methanol oxidation at poly- and  
647 monocrystalline platinum electrodes: The effect of anion, temperature, surface structure,  
648 Ru adatom, and potential, *J. Phys. Chem. C*, 2007, **111**, 7038–7048.  
649 8 J. Shin and C. Korzeniewski, Infrared spectroscopic detection of CO formed at step and  
650 terrace sites on a corrugated electrode surface plane during methanol oxidation, *J. Phys.*  
651 *Chem.*, 1995, **99**, 3419–3422.  
652 9 T. H. M. Housmans and M. T. M. Koper, Methanol Oxidation on Stepped Pt[ n (111) ×  
653 (110)] Electrodes: A Chronoamperometric Study, *J. Phys. Chem. B*, 2003, **107**, 8557–  
654 8567.  
655 10 V. Grozovski, V. Climent, E. Herrero and J. M. Feliu, The role of the surface structure in  
656 the oxidation mechanism of methanol, *J. Electroanal. Chem.*, 2011, **662**, 43–51.  
657 11 A. Testolin, S. Cattaneo, W. Wang, D. Wang, V. Pifferi, L. Prati, L. Falciola and A. Villa,  
658 Cyclic Voltammetry Characterization of Au, Pd, and AuPd Nanoparticles Supported on  
659 Different Carbon Nanofibers, *Surfaces*, 2019, **2**, 205–215.  
660 12 H. Varela, M. V. F. Delmonde and A. A. Zülke, in *Electrocatalysts for Low Temperature*  
661 *Fuel Cells: Fundamentals and Recent Advancements*, eds. T. Maiyalagan and V. S. Sagi,  
662 Wiley-VCH Verlag GmbH & Co. KGaA, Weinheim, Germany, 2017, pp. 145–163.  
663 13 M. Hachkar, B. Beden and C. Lamy, Oscillating electrocatalytic systems. Part I. Survey of  
664 systems involving the oxidation of organics and detailed electrochemical investigation of  
665 formaldehyde oxidation on rhodium electrodes, *J. Electroanal. Chem.*, 1990, **287**, 81–98.  
666 14 K. Krischer and H. Varela, in *Handbook of Fuel Cells*, eds. W. Vielstich, A. Lamm and H.  
667 A. Gasteiger, John Wiley & Sons, Ltd, Chichester, UK, 2010, vol. 2, pp. 679–701.  
668 15 U. Krewer, T. Vidakovic-Koch and L. Rihko-Struckmann, Electrochemical oxidation of  
669 carbon-containing fuels and their dynamics in low-temperature fuel cells, *ChemPhysChem*,  
670 2011, **12**, 2518–2544.  
671 16 E. G. Machado and H. Varela, in *Encyclopedia of Interfacial Chemistry*, Elsevier, 2018,  
672 pp. 701–718.

- 673 17 M. Krausa, W. Vielstich, M. Kraus and W. Vielstich, Potential oscillations during  
674 methanol oxidation at Pt-electrodes Part 1: experimental conditions, *J. Electroanal. Chem.*,  
675 1995, **399**, 7–12.
- 676 18 H. Okamoto, N. Tanaka and M. Naito, Chaos in the oxidation of formaldehyde and/or  
677 methanol, *J. Phys. Chem. A*, 1997, **101**, 8480–8488.
- 678 19 M. V. F. Delmonde, M. A. Nascimento, R. Nagao, D. A. Cantane, F. H. B. Lima and H.  
679 Varela, Production of volatile species during the oscillatory electro-oxidation of small  
680 organic molecules, *J. Phys. Chem. C*, 2014, **118**, 17699–17709.
- 681 20 R. Nagao, R. G. Freitas, C. D. Silva, H. Varela and E. C. Pereira, Oscillatory electro-  
682 oxidation of methanol on nanoarchitected Ptpc/Rh/Pt metallic multilayer, *ACS Catal.*,  
683 2015, **5**, 1045–1052.
- 684 21 J. Lee, C. Eickes, M. Eiswirth and G. Ertl, Electrochemical oscillations in the methanol  
685 oxidation on Pt, *Electrochim. Acta*, 2002, **47**, 2297–2301.
- 686 22 A. L. Martins, B. C. Batista, E. Sitta and H. Varela, Oscillatory instabilities during the  
687 electrocatalytic oxidation of methanol on platinum, *J. Braz. Chem. Soc.*, 2008, **19**, 679–  
688 687.
- 689 23 E. A. Carbonio, R. Nagao, E. R. Gonzalez and H. Varela, Temperature effects on the  
690 oscillatory electro-oxidation of methanol on platinum, *Phys. Chem. Chem. Phys.*, 2009, **11**,  
691 665–670.
- 692 24 S. Sauerbrei, M. A. Nascimento, M. Eiswirth and H. Varela, Mechanism and model of the  
693 oscillatory electro-oxidation of methanol, *J. Chem. Phys.*, 2010, **132**, 1–10.
- 694 25 R. Nagao, E. Sitta and H. Varela, Stabilizing nonstationary electrochemical time series, *J.*  
695 *Phys. Chem. C*, 2010, **114**, 22262–22268.
- 696 26 E. Boscheto, B. C. Batista, R. B. Lima and H. Varela, A surface-enhanced infrared  
697 absorption spectroscopic (SEIRAS) study of the oscillatory electro-oxidation of methanol  
698 on platinum, *J. Electroanal. Chem.*, 2010, **642**, 5.
- 699 27 R. Nagao, D. A. Cantane, F. H. B. Lima and H. Varela, The dual pathway in action:  
700 decoupling parallel routes for CO<sub>2</sub> production during the oscillatory electro-oxidation of  
701 methanol, *Phys. Chem. Chem. Phys.*, 2012, **14**, 5.
- 702 28 R. Nagao, D. A. Cantane, F. H. B. Lima and H. Varela, Influence of anion adsorption on  
703 the parallel reaction pathways in the oscillatory electro-oxidation of methanol, *J. Phys.*  
704 *Chem. C*, 2013, **117**, 15098–15105.
- 705 29 B. A. F. Previdello, P. S. Fernández, G. Tremiliosi-Filho and H. Varela, Oscillatory  
706 Electro-oxidation of Methanol on Platinum Single Crystal Electrodes, *Electrocatalysis*,  
707 2016, **7**, 276–279.
- 708 30 B. A. F. Previdello, P. S. Fernández, G. Tremiliosi-Filho and H. Varela, Probing the  
709 surface fine structure through electrochemical oscillations, *Phys. Chem. Chem. Phys.*,  
710 2018, **20**, 5674–5682.
- 711 31 J. Clavilier, D. Armand, S. G. Sun and M. Petit, Electrochemical adsorption behaviour of  
712 platinum stepped surfaces in sulphuric acid solutions, *J. Electroanal. Chem.*, 1986, **205**,  
713 267–277.
- 714 32 B. Lang, R. W. Joyner and G. A. Somorjai, Low energy electron diffraction studies of high  
715 index crystal surfaces of platinum, *Surf. Sci.*, 1972, **30**, 440–453.
- 716 33 J. Clavilier, K. E. Actii, M. Petit, A. Rodes and M. A. Zamakhchari, Electrochemical  
717 monitoring of the thermal reordering of platinum single-crystal surfaces after  
718 metallographic polishing from the early stage to the equilibrium surfaces, *J. Electroanal.*  
719 *Chem. Interfacial Electrochem.*, 1990, **295**, 333–356.
- 720 34 V. Del Colle, A. Berná, G. Tremiliosi-Filho, E. Herrero and J. M. Feliu, Ethanol  
721 electrooxidation onto stepped surfaces modified by Ru deposition: Electrochemical and  
722 spectroscopic studies, *Phys. Chem. Chem. Phys.*, 2008, **10**, 3766–3773.



- 723 35 V. Del Colle, J. Souza-Garcia, G. Tremiliosi-Filho, E. Herrero and J. M. Feliu,  
724 Electrochemical and spectroscopic studies of ethanol oxidation on Pt stepped surfaces  
725 modified by tin adatoms, *Phys. Chem. Chem. Phys.*, , DOI:10.1039/c1cp20546c.
- 726 36 A. F. B. B. Barbosa, V. Del Colle, A. M. Gómez  
727 Filho, A. M. Gómez-Marín, C. A. Angelucci and G. Tremiliosi-Filho, Effect of the  
728 Random Defects Generated on the Surface of Pt(111) on the Electro-oxidation of Ethanol:  
729 An Electrochemical Study, *ChemPhysChem*, 2019, **20**, 3045–3055.
- 730 37 F. Colmati, G. Tremiliosi-Filho, E. R. Gonzalez, A. Berná, E. Herrero and J. M. Feliu,  
731 Surface structure effects on the electrochemical oxidation of ethanol on platinum single  
732 crystal electrodes, *Faraday Discuss.*, 2008, **140**, 379–397.
- 733 38 V. Briega-Martos, E. Herrero and J. M. Feliu, Pt(hkl) surface charge and reactivity, *Curr.*  
734 *Opin. Electrochem.*, 2019, **17**, 97–105.
- 735 39 R. Gómez, V. Climent, J. M. Feliu and M. J. Weaver, Dependence of the Potential of Zero  
736 Charge of Stepped Platinum (111) Electrodes on the Oriented Step-Edge Density:  
737 Electrochemical Implications and Comparison with Work Function Behavior, *J. Phys.*  
738 *Chem. B*, 2000, **104**, 597–605.
- 739 40 Y. Mukouyama, O. Furuyama, Y. Bundo and H. Okamoto, Separate Current Range for  
740 Appearance of Potential Oscillation during Methanol Oxidation on Platinum,  
741 *Electrochemistry*, 2014, **82**, 573–577.
- 742 41 M. F. Cabral, R. Nagao, E. Sitta, M. Eiswirth and H. Varela, Mechanistic aspects of the  
743 linear stabilization of non-stationary electrochemical oscillations, *Phys. Chem. Chem.*  
744 *Phys.*, 2013, **15**, 1437–1442.
- 745 42 N. Perini, B. C. Batista, A. C. D. D. C. Angelo, I. R. Epstein and H. Varela, Long-lasting  
746 oscillations in the electro-oxidation of formic acid on PtSn intermetallic surfaces,  
747 *ChemPhysChem*, 2014, **15**, 8.
- 748 43 N. Perini, E. Sitta, A. C. D. Angelo and H. Varela, Electrocatalytic activity under  
749 oscillatory regime: The electro-oxidation of formic acid on ordered Pt3Sn intermetallic  
750 phase, *Catal. Commun.*, 2013, **30**, 23–26.
- 751 44 G. Samjeské, A. Miki, S. Ye, A. Yamakata, Y. Mukouyama, H. Okamoto and M. Osawa,  
752 Potential oscillations in galvanostatic electrooxidation of formic acid on platinum: A time-  
753 resolved surface-enhanced infrared study, *J. Phys. Chem. B*, 2005, **109**, 23509–23516.
- 754 45 G. B. Melle, F. W. Hartl, H. Varela and E. Sitta, The effect of solution pH on the  
755 oscillatory electro-oxidation of methanol, *J. Electroanal. Chem.*, 2018, **826**, 164–169.
- 756 46 E. A. Batista, G. R. P. Malpass, A. J. Motheo and T. Iwasita, New insight into the  
757 pathways of methanol oxidation, *Electrochem. commun.*, 2003, **5**, 843–846.
- 758 47 E. A. Batista, G. R. P. Malpass, A. J. Motheo and T. Iwasita, New mechanistic aspects of  
759 methanol oxidation, *J. Electroanal. Chem.*, 2004, **571**, 273–282.
- 760 48 H. Wang, T. Löffler and H. Baltruschat, Formation of intermediates during methanol  
761 oxidation: A quantitative DEMS study, *J. Appl. Electrochem.*, 2001, **31**, 759–765.
- 762 49 M. J. T. C. Van Der Niet, N. Garcia-Araez, J. Hernández, J. M. Feliu and M. T. M. Koper,  
763 Water dissociation on well-defined platinum surfaces: The electrochemical perspective,  
764 *Catal. Today*, 2013, **202**, 105–113.
- 765 50 M. J. S. Farias, G. A. Camara and J. M. Feliu, Understanding the CO Preoxidation and the  
766 Intrinsic Catalytic Activity of Step Sites in Stepped Pt Surfaces in Acidic Medium, *J. Phys.*  
767 *Chem. C*, 2015, **119**, 20272–20282.
- 768 51 A. Calderón-Cárdenas, F. W. Hartl, J. A. C. Gallas and H. Varela, Modeling the triple-path  
769 electro-oxidation of formic acid on platinum: Cyclic voltammetry and oscillations, *Catal.*  
770 *Today*, 2020, in press.
- 771 52 J. G. Freire, A. Calderón-Cárdenas, H. Varela and J. A. C. Gallas, Phase diagrams and  
772 dynamical evolution of the triple-pathway electro-oxidation of formic acid on platinum,

-Marín, C. A. Angelucci, G. Tremiliosi-Filho

773  
774

*Phys. Chem. Chem. Phys.*, 2020, **22**, 1078–1091.